

The Wave Exciting Forces Acting on a Submerged-Plate

Sang-Min Lee* · Gil-Young Kong** · Chol-Seong Kim***

*,**Dept. of Ship Operation Systems Engineering, Korea Maritime University, Pusan 606-791, Korea

***Div. of Maritime Transportation System, Mokpo National Maritime University, Mokpo 530-729, Korea

ABSTRACT : In this study, we focus on the submerged plate built into the Very Large Floating Structure with the partial openings of 5m long, which enables the reverse flow of incident wave to generate the wave breaking. The purpose of this study is to investigate the characteristics of wave exciting forces acting on the submerged plate. Firstly, we have carried out the extensive experiments to understand the characteristics of the wave exciting forces. Then we have performed the numerical simulations by applying the Marker and Cell method and compare with the experimental results. We discuss the validity of MAC method and the effects of the submerged plate on the motion of VLFS.

KEY WORDS : Wave exciting forces, Submerged-plate, Marker and Cell method

1. Introduction

Ocean space utilization has been considered as one of the most important subjects related to ocean development in Japan. A concept of construction of large scale artificial islands by using a Very Large Floating Structure (VLFS) has been attractive during these thirty years. Under these circumstances, a pontoon type floating structure named as Mega-Float was installed in Tokyo Bay in 1995 and a number of measurements were conducted (Yoshida, 2003). Hydroelastic response of pontoon type floating structure in waves is critical in structural design. Therefore the conventional Mega-Float is only set up in relatively calm water behind islands or breakwaters. Hence, it is necessary to develop a new technology that make be possible to install VLFS to deeper water fields in order to make use of the characteristics as a floating structure. Takaki *et al.* have studied the performance of the breakwater systems experimentally and theoretically using the submerged horizontal plate (Takaki and Lin, 2000). The basic mechanism of dissipating wave energy was shown in Takaki's studies. Namely, when the incident wave propagates into the submerged plate, the flow due to the wave is accelerated

around the fore edge of the plate, while strong reverse flow is generated at the aft edge. These two opposite flows collide each other, as a results, wave breaking and wave fission dissipates the incident wave energy. The performance of the submerged plate type breakwater was found to be quite sensitive to the submerged depth. In this study, we focus on the submerged plate built into the VLFS with the partial openings of 5m long, which enables the reverse flow of incident wave to generate the wave breaking. This plate mainly contributes to the reduction of short incident waves including those generated by the first and second submerged plate, the upper deck and the tubular frames, are introduced to give enough strength as a wave breaking system. Characteristics of wave exciting forces acting on the submerged plate are investigated in this study. Firstly we have carried out the extensive experiments to make clear the characteristics of the wave exciting forces acting on the submerged plate. Then we perform the numerical simulations by applying the Marker and Cell method (MAC method) and compare with the experimental results. We discuss the validity of MAC method and the effects of the submerged plate on the motion of VLFS.

2. Experimental Tank Test

The experiments were carried out in the two-dimensional wave tank, which is 42 meters in length, 1.2 meters in

*정회원, smlee@bada.hhu.ac.kr 051)410-4868

**정회원, gykong@hhu.ac.kr 051)410-4273

***정회원, cskimu@mail.mmu.ac.kr 061)240-7307

breadth and 2 meters in depth. The submerged plate is supported by four shafts of diameter 10mm. We measured the wave exciting forces for heave acting on the submerged plate. We performed the extensive experiments to understand the characteristics of the wave exciting forces by using the 1/50 scale model of the submerged plate. The principal particulars of the submerged plate and the experimental conditions are shown in Table 1. It also shows the actual sea conditions corresponding to the experimental conditions. The tests were done every 0.141 seconds from the period of 0.989 to 2.828 seconds in regular waves with the wave amplitude of 10mm and 30mm, respectively. These experimental data were analyzed by means of Fourier series. The components from the first to the fifth order are shown in the figures.

Table1. Principal particulars of submerged plate and experimental conditions

	Actual plate	Model[1/50]
Water depth	100m	2m
Length of plate	30m	600mm
Thickness of plate	1m	20mm
Submerged depth of plate	2m	40mm
Wave amplitude	0.5m, 1.5m	10mm, 30mm
Wave period	7-20sec (every 1sec)	0.989-2.828sec (every 0.141sec)

The non-dimensional forms of the wave exciting forces are as follows

$$\text{Heaving force} : \hat{F}_z = F_z / \rho g \zeta_a B L \quad (1)$$

where, the symbols ρ , g , ζ_a , L , and B are the fluid density, gravity acceleration, wave amplitude, length of submerged plate, and breadth of submerged plate.

3. Numerical Scheme

3.1 Computational procedure

We have performed the numerical simulation based on the MAC method. The governing equations which are the Navier-Stokes equation and the continuity equation in the case of two-dimensional, incompressible and viscous fluid are represented as follows,

$$\frac{\partial u}{\partial x} + \frac{\partial w}{\partial z} = 0 \quad (2)$$

$$\frac{\partial u}{\partial t} + u \frac{\partial u}{\partial x} + w \frac{\partial u}{\partial z} = -\frac{\partial \phi}{\partial x} + \nu \left(\frac{\partial^2 u}{\partial x^2} + \frac{\partial^2 u}{\partial z^2} \right) \quad (3)$$

$$\frac{\partial w}{\partial t} + u \frac{\partial w}{\partial x} + w \frac{\partial w}{\partial z} = -\frac{\partial \phi}{\partial z} + \nu \left(\frac{\partial^2 w}{\partial x^2} + \frac{\partial^2 w}{\partial z^2} \right) + g \quad (4)$$

Here the Cartesian coordinate system (x, y) is employed

and velocity components are u, w in respective direction. ϕ is the pressure divided by the fluid density and ν is the kinematic viscosity. The computational domain is discretized into a staggered rectangular inflexible mesh system, with constant spacing in the horizontal direction while variable in the vertical one in order to have finer mesh near the body and the free surface.

The calculation proceeds through a sequence of loops each advancing the entire flow configuration through sufficiently small time increments Δt which satisfy the stability criteria posed by Courant Number. An Euler explicit time stepping scheme is used for the time marching procedure.

The pressure field at the n -th time step is obtained by iteratively solving the following Poisson equation which is derived by taking the divergence of velocities and set it to zero at the $(n+1)$ th time step.

The Poisson equation is solved as the boundary value problem by the Successive Over Relaxation (SOR) method except in the boundary cells, and it is iteratively solved by using

$$\Phi^{m+1} = \Phi^m + \omega \cdot (\Phi_{cal}^{m+1} - \Phi^m) \quad (5)$$

where ω represents the relaxation factor and superscript indicate the number of iteration. Iterations are stopped when the pressure difference between two consecutive approximations is smaller than a certain quantity ϵ , chosen in advance. The N-S equations (3) and (4) are hyperbolic equations to be solved as an initial value problem, while the Poisson equation is an elliptic equation to be solved as a boundary value problem. The cycle is repeated until the number of time steps reaches the predetermined value.

The finite-difference scheme for the convective terms must be carefully chosen, since it often renders decisive influences on the results. In this study, a third-order upwind scheme with variable mesh size is employed for the fluid domains. In the vicinity of the boundaries, where sufficient numbers of velocity points are not available, the combination of a second-order centered and donor cell scheme is used depending on the number of available velocity points. On the other hand, the second-order centered scheme is employed for the diffusive terms. The second-order Adams-Bashforth method is used for the time differencing.

3.2 Free-surface condition

The dynamic and kinematic free-surface conditions are written as

$$\phi = \phi_0 = 0 \quad \text{on } z = \eta \quad (6)$$

$$\frac{D(\eta - z)}{Dt} = 0 \quad \text{on } z = \eta \quad (7)$$

where η is wave height and ϕ_0 is the atmospheric pressure

divided by the density of fluid. The viscous stress and surface tension on the free-surface are neglected in this study. As it was already proved by Hinatsu (Hinatsu, 1992), the tangential stress at the free-surface affects the results extremely slightly and it can be neglected for the flow around the body.

The dynamic condition expressed by Eq.(6) is fulfilled in the procedure of pressure computation described below, and the kinematic condition expressed by Eq.(7) is fulfilled by the *Lagrangian* movement of the segments that form the free-surface configuration. The two end-points of each segment are located on the underlying lines of the rectangular cell system. Since their coordinates are defined in two dimensions, this use of segments enables the expression of a free-surface configuration. The end-points of the segments are moved in the following *Lagrangian* manner like the marker particles of the MAC method (Welch et al., 1966),

$$\begin{aligned} x^{n+1} &= x^n + \Delta t \cdot u \\ z^{n+1} &= z^n + \Delta t \cdot w \end{aligned} \quad (8)$$

Here, (x^n, z^n) is the location of the end points of the old segment and the new segment is temporarily determined by (x^{n+1}, z^{n+1}) . Then, the new end-points are determined from the crossings of the temporary segments with the underlying mesh lines. The velocity vector (u, w) for the movement of the end-points is given by linear interpolation from the neighboring velocities.

The dynamic free-surface condition of Eq.(6) is implemented by the irregular star technique (Chan and Street, 1970) in the solution process of the Poisson equation for the pressure. The irregular star technique means that the finite difference formula for Poisson equation was applied for five points spaced irregularly including one or two free-surface nodes where the pressure is the same as atmospheric pressure.

3.3 Boundary conditions

At the inflow boundary of the computational domain, a numerical wavemaker is established by prescribing the inflow velocities based on the linear theory, the inflow velocities are given as follows,

$$u_{\frac{1}{2},k} = \omega \zeta_a \frac{\cosh K(h + ZP_k)}{\sinh(Kh)} \sin\left(\omega t + K \frac{DX}{2}\right) \quad (9)$$

$$w_{\frac{1}{2},k} = \omega \zeta_a \frac{\sinh K\left(h + ZP_k - \frac{1}{2} \frac{DZ_k}{\omega}\right)}{\sinh(Kh)} \cos(\omega t) \quad (10)$$

where ζ_a is the wave amplitude, ω is the angular frequency, K is the wave number and h is the depth of region.

At the bottom boundary of the computational domain, the free-slip boundary conditions are given for the velocity, and the zero-normal gradient condition is imposed for the boundary condition of pressure.

In the present study, the added dissipation zone method is employed as the wave absorbing condition at the outflow boundary. Inside the damping zone, the mesh size is gradually increased in the horizontal direction to provide additional numerical damping.

4. Results and discussion

We have validated the MAC method by the comparison of hydrodynamic forces on the submerged plate with the experimental results. Fig.1 shows the wave exciting forces for heave on the fore part of VLFS with the submerged plate obtained by the present numerical calculations and experiments. Numerical results are in good agreement with not only the experimental ones with the first order component but also the ones with the second and third order components. From this comparison, we can say that the MAC method is a useful tool for estimating the non-linear hydrodynamic forces on the complex formed structure such as the float with the submerged plate.

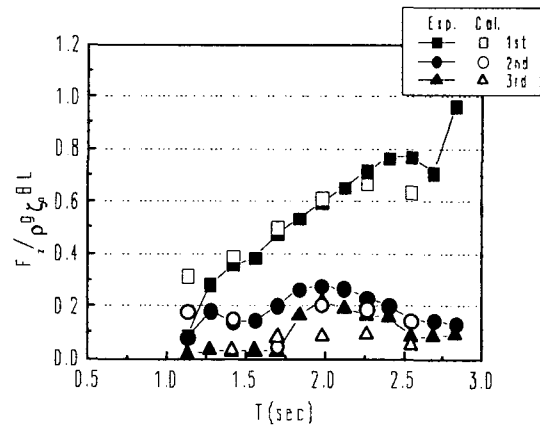


Fig. 1 Wave exciting forces on VLFS with sub-plate ($\zeta_a = 30 \text{ mm}$)

Figs. 2 and 3 show the wave exciting forces for heave acting on the submerged plate built into VLFS. The experimental results show the first order component to the fifth order component. Fig.2 corresponds to the results with the wave amplitude $\zeta_a = 10 \text{ mm}$, and Fig.3 is the results with $\zeta_a = 30 \text{ mm}$.

Even though the violent wave breaking phenomena have occurred above the submerged plate in the experiment, it

has to be noticed that the first order components are dominant in comparison with the ones on VLFS with submerged plate (see Fig.1). Therefore, we may say that the wave fission due to the breaking waves scarcely affects the hydrodynamic forces acting on the submerged plate, and it affects strongly the ones on the structure behind the submerged plate.

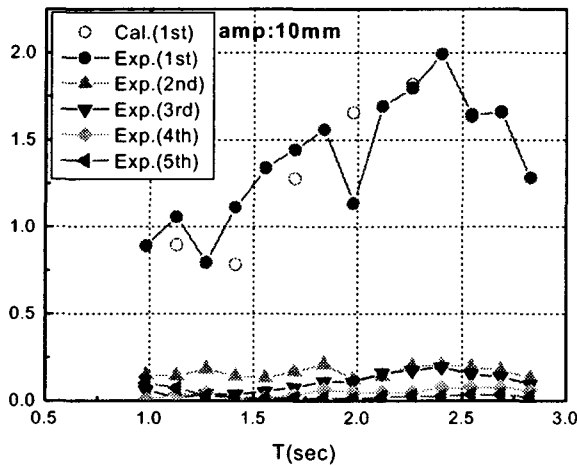


Fig. 2 Wave exciting forces on submerged plate ($\zeta_a = 10\text{mm}$)

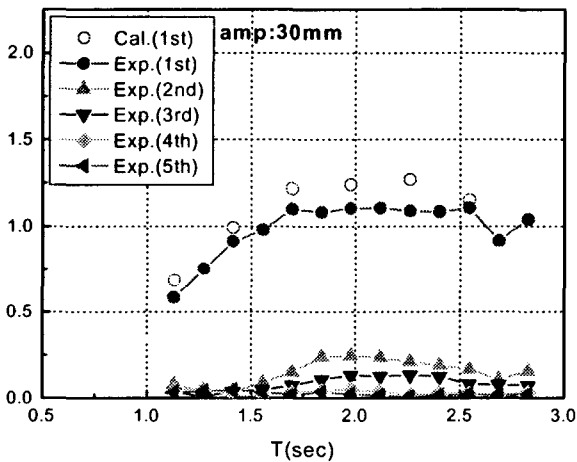


Fig. 3 Wave exciting forces on submerged plate ($\zeta_a = 30\text{mm}$)

The numerical results denoted with the mark of \circ are in good agreement with the experimental ones irrespective of the wave amplitudes, and the wave exciting forces increase with the wave period.

Fig.4 shows the velocity vector fields and pressure contours around the submerged plate without the VLFS corresponding to the short wave period $T_w = 0.8\text{sec}$, submergence depth $d = 20\text{mm}$, and wave amplitude $\zeta_a = 50\text{mm}$. This simulation was performed by using the 1/100 scale model to apply to the hydroelastic response of

VLFS in the case with submerged plate. The characteristic of hydroelastic response is regarded as the characteristic of energy propagation in waves. The energy of propagation wave consists of incident wave energy, reflection wave energy and dissipation wave energy. It is considered that the increase of dissipation wave energy and the decrease of incident wave energy will reduce the energy of the propagation wave. The breaking wave induced by the submerged plate is a typical example of the dissipation wave energy. From this figure, we can observe that the incident wave energy is considerably decreased due to the submerged plate. Therefore, the attachment of additional structure on the weather side of VLFS can bring about the reduction of propagation wave energy. As a result, the submerged plate can be expected to reduce the motion of VLFS in waves.

5. Conclusion

We have carried out the extensive experiments to understand the comprehensive characteristics of wave exciting forces acting on the submerged plate. Furthermore, we have performed the numerical simulation by applying the MAC method. The comparison of the results have shown a good agreement between the numerical calculations and experiments. As a result, it is considered that the MAC method is useful tool for estimating the non-linear hydrodynamic forces acting on the submerged plate.

References

- [1] Chan, R. K. C. and Street, R. L.(1970), "A Computer Study of Finite Amplitude Water Waves", *J. Comput. Phys.*, Vol.6, pp.68-94.
- [2] Hinatsu, M.(1992), "Numerical Simulation of Unsteady Viscous Nonlinear Waves Using Moving Grid System Fitted on a Free Surface", *J. Kansai Soc. Nav. Archt. Japan*, No.217, pp.1-11.
- [3] Takaki, M. and Lin, X.(2000), "Hydrodynamic Forces on a Submerged Horizontal Plate Type Breakwater", *Proc. 10th ISOPE*, Seattle, Vol.III, pp.532-539.
- [4] Welch, J. E., Harlow, F. H., Shabbon, J. P. and Daly, B. J.(1966), "The MAC Method a Computing Technique for Solving Viscous, Incompressible, Transient Fluid Flow Problems Involving Free Surface", *Los Alamos Scientific Laboratory Report LA-3425*, Los Alamos, New Mexico.
- [5] Yoshida, K.(2003), "A Brief Review of Recent Activities on VLFS in Japan", *Proc. of International Symposium on Ocean Space Utilization Technology*, Tokyo, pp.25-32.

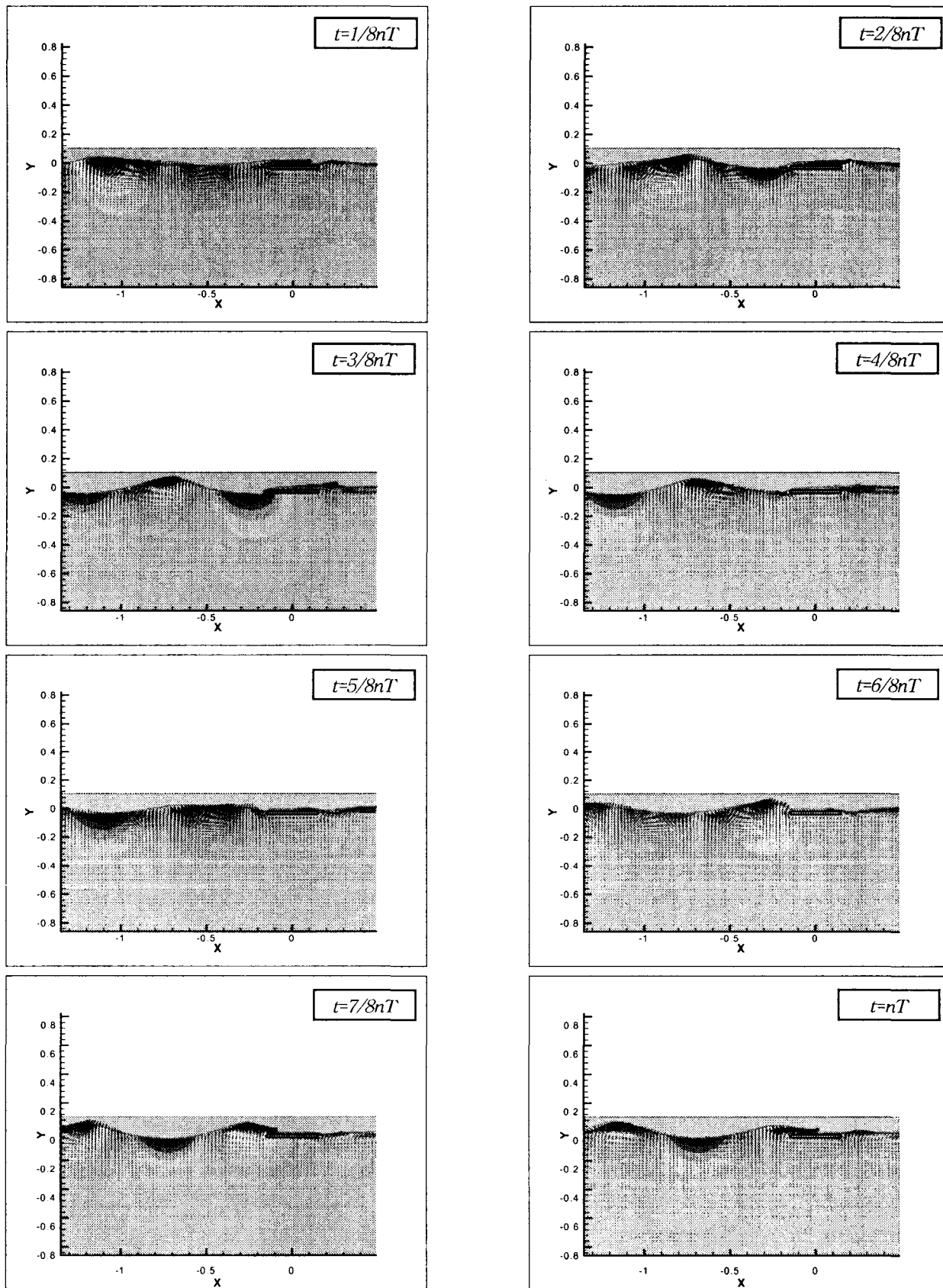


Fig. 4 Velocity vector field and pressure contour for $T_w=0.8\text{sec}$, $\zeta_a=50\text{mm}$